

## Origin of fermion masses without spontaneous symmetry breaking

Venkitesh Ayyar and Shailesh Chandrasekharan

*Department of Physics, Box 90305, Duke University, Durham, North Carolina 27708, USA*

(Received 23 December 2015; published 20 April 2016)

Using large scale Monte Carlo calculations in a simple three dimensional lattice fermion model, we establish the existence of a second order quantum phase transition between a massless fermion phase and a massive one, both of which have the same symmetries. This shows that fermion masses can arise due to dynamics without the need for spontaneous symmetry breaking. Universality suggests that this alternate origin of the fermion mass should be of fundamental interest.

DOI: [10.1103/PhysRevD.93.081701](https://doi.org/10.1103/PhysRevD.93.081701)

Origin of mass in the universe is an interesting problem in fundamental physics [1]. In continuum quantum field theory fermion masses arise from local fermion bilinear mass terms that are introduced as parameters in the theory. If symmetries of the theory prevent such terms, perturbatively fermions remain massless. However, these symmetries can break spontaneously through the formation of nonzero fermion bilinear condensates that can make fermions massive. This mechanism of mass generation is used in the standard model of particle physics to give quarks and leptons their masses. Recent progress in the field of topological insulators suggests the existence of an alternate mechanism for the origin of fermion mass [2–7]. These studies argue that massless fermions can become massive even without the formation of fermion bilinear condensates, at a second order quantum phase transition where there is no spontaneous symmetry breaking. Evidence for such a transition has been found using Monte Carlo calculations on small lattices in complicated models inspired by the physics of electrons hopping on a honeycomb lattice [8,9].

If the existence of the above quantum phase transition can be established firmly in four space-time dimensions, it will provide a fundamentally new mechanism to understand the origin of fermion mass in continuum quantum field theory. The physics of such a transition was proposed long ago as a way to solve the long standing problem of formulating chiral lattice gauge theories [10]. Unfortunately, the transition was never found and the subject was abandoned [11]. The recent insights from the field of topological insulators suggest that such transitions are natural and proposals to construct chiral lattice gauge theories have begun to appear again [12–14]. However, concrete evidence for the transition so far has mostly been provided using models with a condensed matter flavor in three space-time dimensions and through Monte Carlo calculations on small lattices. Given the past history and controversial nature of the second order transition it is important to confirm its existence on large lattices and compute the associated critical exponents. Further, if universality holds the same transition should also be observable in three dimensional lattice field theory models that were studied long ago in the context of high energy

physics. In this work we accomplish both these tasks and thus bridge the gap between the two communities.

Existence of the second order quantum phase transition that we establish in this work is also interesting more broadly. Most phase transitions occur due to a change in the symmetry properties of the ground state, described by fluctuations of a local order parameter associated with the symmetry group. Our transition is different since there is no change in the symmetry between the two phases. All local symmetry order parameters vanish in both the phases. Such exotic transitions between two phases with the same symmetries are believed to be driven due to a change in quantum entanglement and topology of the ground state [15,16]. In certain cases these transitions are accompanied by fractionalization of the fundamental degrees of freedom and emergence of gauge fields [17]. Search for these exotic transitions has become popular lately [18,19]. Unfortunately, many proposals for such transitions suffer from sign problems and are constructed in models relevant to condensed matter physics. Our work shows that a similar transition exists in a simple lattice four-fermion model of interest to high energy physicists. Importantly, the model does not suffer from sign problems. From the point of view of topological insulators, our transition is between a semimetal and a trivial insulator, very similar to the one proposed recently in [8,9], but within a much simpler model.

Our model can be motivated from lattice Higgs-Yukawa models in the limit where bosons are heavy and can be integrated out yielding a four-fermion interaction [20–23]. The four-fermion model can also be constructed directly by naively discretizing on a cubic space-time lattice, a single continuum four component massless Dirac field theory with a simple four-fermion interaction obtained by multiplying the four Dirac components with each other. Since the interaction binds four fermion fields together into a local singlet at each space-time lattice site, a massive fermion phase (a trivial insulator) emerges at strong couplings where no symmetries are spontaneously broken. This phase has the same lattice symmetries as the massless fermion phase at weak couplings (a semimetal). Earlier studies found that the two phases were separated by a more conventional spontaneously broken phase, shown as

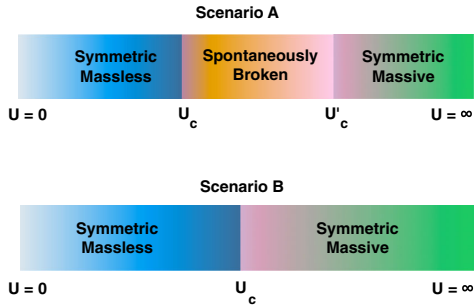


FIG. 1. Two possible scenarios for the phase diagram of lattice models that show the origin of a fermion mass without spontaneous symmetry breaking. The massless and the massive fermion phases have the same symmetries. Previous studies in four space-time dimensions found results consistent with scenario A, while our work in three space-time dimensions is consistent with scenario B with a second order quantum critical point at  $U_c$ .

scenario A in Fig. 1, both in three [24] and four space-time dimensions [22]. Some mean field theory calculations predicted a direct first order transition [25,26]. Absence of a direct second order transition was taken as evidence that the massive fermion phase was simply a lattice artifact. However, we find clear evidence for a direct second order transition between the two phases in three space-time dimensions. This is shown as scenario B in Fig. 1.

Large lattice calculations are essential to confirm the transition given that it separates two phases with the same symmetries and does not fall under the usual Landau-Ginzburg paradigm. Unfortunately, fermion algorithms are known to scale poorly with system size, especially near a critical point. Recently we discovered that in the fermion bag approach [27,28], with sufficient memory, the information necessary to perform all updates can be stored. Using this idea we can perform fast updates within large regions of space-time and update a  $60^3$  lattice within about five hours on a single CPU core and a memory of about 8 GB. Such large scale calculations are unprecedented and help us establish the nature of the phase transition firmly and compute its properties. Some other technical details of our work on small lattices have already appeared earlier in [29] and have been verified recently in [30]. But the broad ramifications of our work across fields have so far remained unappreciated.

Our model contains four flavors of massless reduced lattice staggered fermions on a cubical space-time lattice with an onsite four-fermion interaction. Each lattice fermion flavor describes a single four-component Dirac fermion in the continuum due to fermion doubling [31–33]. The model can be obtained from a Higgs-Yukawa model in the limit where the Higgs field hopping term vanishes [22,23]. We also believe that our model has a Hamiltonian formulation very similar to the honeycomb lattice models studied recently, but with much simpler interactions [8,9]. We use four-component Grassmann valued fields,  $\psi_{x,i}$ ,  $i = 1, 2, 3, 4$ ,

on each lattice site  $x$  to describe the fermion fields. Then, the Euclidean action of our model is given by:

$$S = \frac{1}{2} \sum_{i=1}^4 \sum_{x,y} \psi_{x,i} M_{x,y} \psi_{y,i} - U \sum_x \psi_{x,1} \psi_{x,2} \psi_{x,3} \psi_{x,4} \quad (1)$$

where  $M$  is the well-known massless staggered fermion matrix given by

$$M_{x,y} = \sum_{\hat{\alpha}=1,2,3} \frac{\eta_{x,\hat{\alpha}}}{2} [\delta_{x,y+\hat{\alpha}} - \delta_{x,y-\hat{\alpha}}], \quad (2)$$

where  $\eta_{x,\hat{\alpha}}$  are phases that introduce a  $\pi$ -flux through all plaquettes. In our work we study cubical lattices of equal size  $L$  in each direction with antiperiodic boundary conditions. Observables are defined as usual through the Grassmann integral

$$\langle \mathcal{O} \rangle = \frac{1}{Z} \int \left( \prod_{i,x} [d\psi_{x,i}] \right) \mathcal{O} e^{-S}. \quad (3)$$

where  $Z$  is the partition function.

The action given in Eq. (1) is symmetric under the usual space-time lattice transformations and an internal  $SU(4)$  flavor transformations [29]. Using weak coupling and strong coupling perturbation theory, it is easy to argue that all lattice symmetries remain unbroken at both weak and strong couplings. Thus, the essential question is whether there is a single transition between the two phases or is there an intermediate phase where some of the lattice symmetries are broken. Previous studies in four space-time dimensions do seem to find such an intermediate phase. Here we present clear evidence from large lattices for a single second order transition between the two phases in three space-time dimensions and estimate the critical exponents at the transition.

We perform calculations using the fermion bag approach [27] where the problem is converted into a statistical mechanics of monomer configurations  $[n]$ , defined through a binary lattice field  $n_x = 0, 1$  which denotes the absence or presence of a monomer at the site  $x$  respectively. Figure 2 shows an illustration of a monomer configuration on a two dimensional lattice. Each monomer represents a four-fermion interaction and free fermions hop on sites that do not contain monomers. The fermion bag approach also gives a very intuitive picture of the underlying physics: At small couplings the monomer density is small and fermions are essentially free, while at strong couplings the lattice is filled with monomers with very few empty sites for free fermions to hop making them massive. Details of our computational approach, including algorithms that we use can be found in [29].

In our earlier work we presented evidence for a single continuous phase transition between the massless

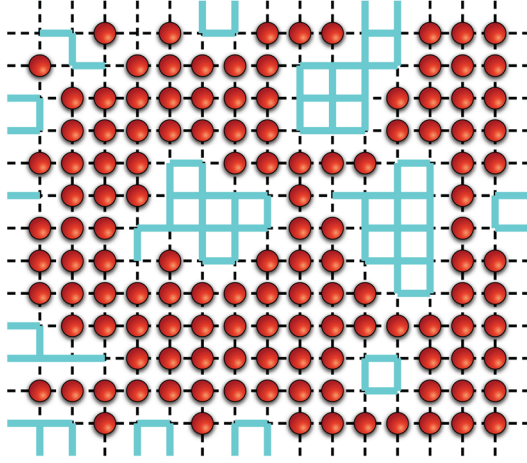


FIG. 2. An example of a monomer configuration  $[n]$  showing free fermion bags on a two dimensional lattice. The filled circles represent monomers and the connected regions without monomers form free fermion bags.

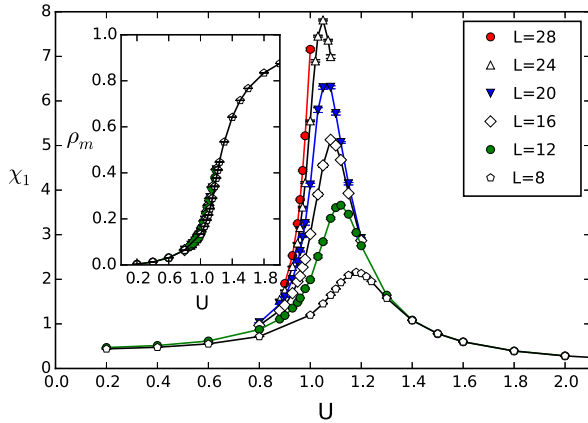


FIG. 3. Plots of  $\rho_m$  and  $\chi_1$  as a function of  $U$  for various values of  $L$ . The susceptibility shows a peak and the average monomer density shows a sharp rise at the phase boundary ( $U \sim 1$ ).

and the massive phases up to lattice sizes of  $L = 28$ . The main result is summarized in Fig. 3 where we plot the monomer density  $\rho_m = U \sum_x \langle \psi_{x,1} \psi_{x,2} \psi_{x,3} \psi_{x,4} \rangle / L^3$  and one of the fermion bilinear susceptibilities  $\chi_1 = \sum_x \langle \psi_{0,1} \psi_{0,2} \psi_{x,1} \psi_{x,2} \rangle$ , as a function of  $U$  for various

TABLE I. Fit results obtained by fitting both  $R_1$  and  $R_2$  to the form  $1/L^{1+\eta}$  for various values of  $U$ . For small  $U$  we approach  $\eta \approx 3$  consistent with the free theory, while in the critical region  $0.93 < U < 0.96$  we again find good fits with a different  $\eta$ .

$U$	$\eta$	$\chi^2/\text{DOF}$	$U$	$\eta$	$\chi^2/\text{DOF}$
0.000	3	...	0.850	2.34(4)	2.5
0.920	1.64(5)	4.6	0.930	1.44(3)	1.9
0.940	1.22(2)	1.0	0.945	1.00(2)	0.7
0.950	0.77(2)	1.1	0.960	0.63(5)	6.4

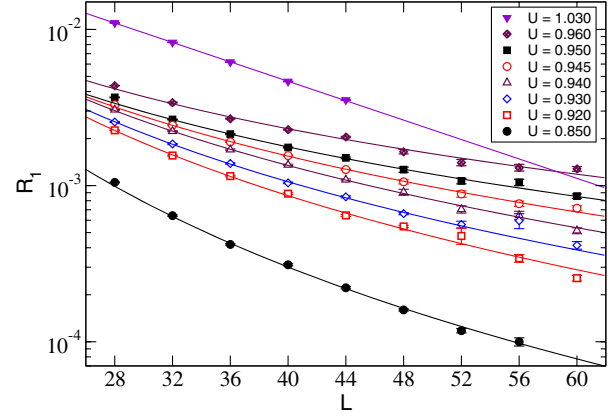


FIG. 4. Plot of  $R_1$  as a function of  $L$  for various values of  $U$  near the critical region. The solid lines are fits to the form  $1/L^{1+\eta}$  where  $\eta$  values are given in Table I, except at  $U = 1.03$  where the solid line has the form  $\exp(-0.07L)$  suggesting the fermions are already massive.

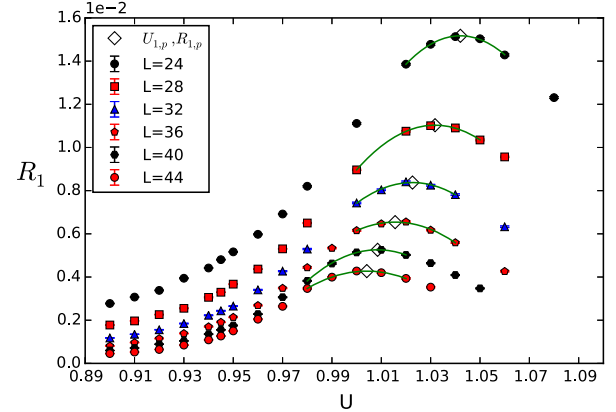


FIG. 5. Plots of  $R_1$  as a function of  $U$  for various lattice sizes showing peaks. The values of the peaks  $R_{1,p}$  and their locations  $U_{1,p}$  are also marked. These are determined by approximating the function to be a quadratic near the maximum.

values of  $L$ . The behavior of these observables is consistent with a single phase transition around  $U \approx 1$ . Most importantly, the bilinear susceptibility never increases like  $L^3$  showing the absence of any local fermion bilinear condensate for all values of  $U$ . Recently it was also confirmed that other discrete lattice symmetries, like the shift symmetry, also remain unbroken for all values of  $U$  [30].

We now have results from much larger lattices (up to  $L = 60$ ) that further confirm a single second order transition. We can also roughly estimate the critical exponents if we assume the absence of corrections to scaling on lattices above  $L = 36$ . Here we focus on the two independent bosonic correlation functions  $C_1(0, x) = \langle \psi_{0,1} \psi_{0,2} \psi_{x,1} \psi_{x,2} \rangle$  and  $C_2(0, x) = \langle \psi_{0,1} \psi_{0,2} \psi_{x,3} \psi_{x,4} \rangle$  where  $x$  is varied along the time direction. Near the critical point both these correlation functions are comparable to each

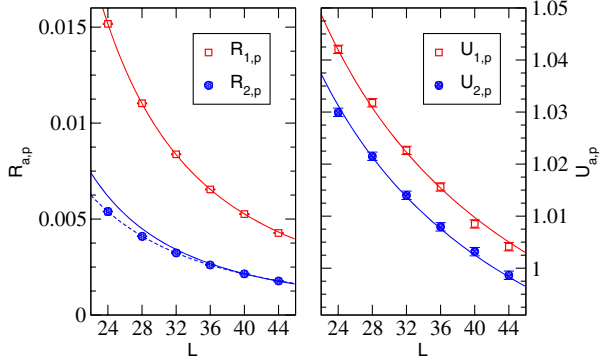


FIG. 6. Plots of  $R_{1,p}$  and  $R_{2,p}$  as a function of  $L$  (left figure) and  $U_{1,p}$  and  $U_{2,p}$  as a function of  $L$ . The solid lines represent fits to the form  $R_{a,p} = b_a/L^{1+\eta}$  and  $U_{a,p} = U_c + d_a/L^\nu$  with  $U_c = 0.943$  fixed. The dashed line is a fit including correction to scaling of the form  $R_{2,p} = b_2/L^{1+\eta} + c_2/L^{1+\eta+\omega}$ , where  $\omega \approx 1$ .

other, while  $C_2(0, x)$  vanishes at  $U = 0$ . For the purpose of comparing different lattice sizes, we extract the correlation ratios  $R_1 = C_1(0, \frac{L}{2} - 1)/C_1(0, 1)$  and  $R_2 = C_2(0, \frac{L}{2})/C_2(0, 0)$  as a function of  $L$ . For large  $L$ , these ratios are expected to scale as  $1/L^4$  in the massless phase, as  $1/L^{1+\eta}$  at the critical point and as  $\exp(-mL)$  in the massive phase. Here  $\eta$  is one of the standard critical exponents. Our data is consistent with this behavior for  $L \geq 32$ . In Table I we show the combined fit results of our data to the form  $1/L^{1+\eta}$  near the critical region. As an illustration of the goodness of our fits, in Fig. 4 we plot  $R_1$  as a function of  $L$  along with the fits. Based on this we estimate that the critical point is somewhere in the region  $0.930 < U < 0.96$ . For  $U \geq 0.96$  a single power law no longer fits the data well, but an exponential fit begins to work well. For example, a fit to the form  $R_1 \sim \exp(-0.07L)$  at  $U = 1.03$  is shown in Fig. 4.

In order to locate  $U_c$  accurately, we analyzed a different scaling region of  $U$  where  $R_1, R_2$  show a peak. In Fig. 5 we plot the behavior of the correlation ratio  $R_1$  as a function of the coupling  $U$  for different lattices sizes [34]. We have computed the maximum values  $R_{1,p}(L), R_{2,p}(L)$  and their locations  $U_{1,p}(L), U_{2,p}$  in the range  $24 \leq L \leq 44$ . From scaling theory, we expect  $R_{a,p} = b_a/L^{1+\eta}$  and  $U_{a,p} = U_c + d_a/L^\nu$ . We find that  $R_{1,p}$  fits well to this expected form for  $24 \leq L \leq 44$ , while  $R_{2,p}$  does not. However if we keep only the data from the largest lattices for both  $R_{1,p}$  and  $R_{2,p}$  we can again perform combined fits to the expected scaling form without the need for corrections to scaling. Interestingly, allowing a scaling correction only for  $R_{2,p}$  allows us to fit the entire data set. Two of these fits are shown in the left plot of Fig. 6. Using these fits and including various systematic errors we estimate  $\eta =$

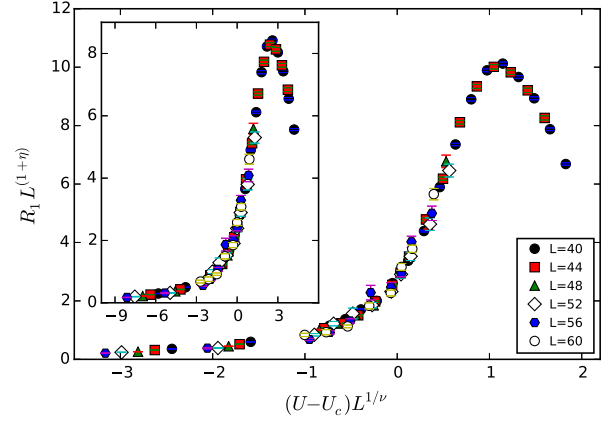


FIG. 7. Evidence for universal scaling in our large lattice data with  $U_c = 0.943$ ,  $\eta = 1.08$ , and  $\nu = 1.30$ . Our data may also be consistent with  $U_c = 0.945$ ,  $\eta = 1$ , and  $\nu = 1$  expected from large  $N$  analysis (shown in the inset), but only after including corrections to scaling.

1.05(5). Combining this result with that of Table I, we constrain  $U_c = 0.943(2)$ . Using this result along with our data for  $U_{a,p}$  and its expected scaling form we can again perform combined fits to obtain  $\nu$ . One such fit is shown in the right plot of Fig. 6. Using these fits we estimate  $\nu = 1.30(7)$ . In Fig. 7 we verify if our large lattice data falls on a single universal scaling function when we fix  $U_c = 0.943$ ,  $\eta = 1.05$  and  $\nu = 1.30$ . The fact that the data falls on a single curve gives us confidence that this is indeed the case. However, we must note that if we allow for scaling corrections to be present in our fits we cannot rule out  $U_c = 0.945$ ,  $\eta = 1.0$  and  $\nu = 1.0$  as expected from large  $N$  four-fermion models [35]. The universal scaling with these exponents is shown in the inset of Fig. 7.

To summarize, we have established the existence of a three dimensional exotic second order phase transition between a massless and a massive fermion phase, both of which have the same lattice symmetries. Such a transition implies that fermion mass generation can be a dynamical phenomenon not necessarily driven by spontaneous symmetry breaking. Such transitions may also exist in four space-time dimensions.

The material presented here is based upon work supported by the U.S. Department of Energy, Office of Science, Nuclear Physics program under Award No. DE-FG02-05ER41368. An important part of the computations performed in this research was done using resources provided by the Open Science Grid [36,37], which is supported by the National Science Foundation and the U.S. Department of Energy's Office of Science.

- [1] F. Wilczek, *Central Eur. J. Phys.* **10**, 1021 (2012).
- [2] A. Kitaev, *AIP Conf. Proc.* **1134**, 22 (2009).
- [3] L. Fidkowski, X. Chen, and A. Vishwanath, *Phys. Rev. X* **3**, 041016 (2013).
- [4] Z.-C. Gu and X.-G. Wen, *Phys. Rev.* **B90**, 115141 (2014).
- [5] M. A. Metlitski, L. Fidkowski, X. Chen, and A. Vishwanath, [arXiv:1406.3032](https://arxiv.org/abs/1406.3032).
- [6] T. Morimoto, A. Furusaki, and C. Mudry, *Phys. Rev. B* **92**, 125104 (2015).
- [7] Y. BenTov, *J. High Energy Phys.* **07** (2015) 034.
- [8] K. Slagle, Y.-Z. You, and C. Xu, *Phys. Rev. B* **91**, 115121 (2015).
- [9] Y.-Y. He, H.-Q. Wu, Y.-Z. You, C. Xu, Z. Y. Meng, and Z.-Y. Lu, [arXiv:1508.06389](https://arxiv.org/abs/1508.06389).
- [10] E. Eichten and J. Preskill, *Nucl. Phys.* **B268**, 179 (1986).
- [11] M. F. Golterman, D. N. Petcher, and E. Rivas, *Nucl. Phys.* **B395**, 596 (1993).
- [12] X.-G. Wen, *Chin. Phys. Lett.* **30**, 111101 (2013).
- [13] Y. You, Y. BenTov, and C. Xu, [arXiv:1402.4151](https://arxiv.org/abs/1402.4151).
- [14] Y.-Z. You and C. Xu, *Phys. Rev. B* **91**, 125147 (2015).
- [15] X. Chen, Z.-C. Gu, Z.-X. Liu, and X.-G. Wen, *Phys. Rev. B* **87**, 155114 (2013).
- [16] T. Senthil, *Annu. Rev. Condens. Matter Phys.* **6**, 299 (2015).
- [17] T. Senthil, A. Vishwanath, L. Balents, S. Sachdev, and M. P. A. Fisher, *Science* **303**, 1490 (2004).
- [18] S. V. Isakov, R. G. Melko, and M. B. Hastings, *Science* **335**, 193 (2012).
- [19] B. Swingle and T. Senthil, *Phys. Rev. B* **86**, 155131 (2012).
- [20] A. Hasenfratz and T. Neuhaus, *Phys. Lett. B* **220**, 435 (1989).
- [21] A. Hasenfratz, W.-q. Liu, and T. Neuhaus, *Phys. Lett. B* **236**, 339 (1990).
- [22] I.-H. Lee, J. Shigemitsu, and R. E. Shrock, *Nucl. Phys.* **B334**, 265 (1990).
- [23] I.-H. Lee, J. Shigemitsu, and R. E. Shrock, *Nucl. Phys.* **B330**, 225 (1990).
- [24] J. L. Alonso, P. Boucaud, V. Martin-Mayor, and A. J. van der Sijs, *Phys. Rev. D* **61**, 034501 (1999).
- [25] M. A. Stephanov and M. Tsy-pin, *Phys. Lett. B* **236**, 344 (1990).
- [26] M. A. Stephanov and M. Tsy-pin, *Phys. Lett. B* **242**, 432 (1990).
- [27] S. Chandrasekharan, *Phys. Rev. D* **82**, 025007 (2010).
- [28] S. Chandrasekharan, *Eur. Phys. J. A* **49**, 90 (2013).
- [29] V. Ayyar and S. Chandrasekharan, *Phys. Rev. D* **91**, 065035 (2015).
- [30] S. Catterall, *J. High Energy Phys.* **01** (2016) 121.
- [31] H. Sharatchandra, H. Thun, and P. Weisz, *Nucl. Phys.* **B192**, 205 (1981).
- [32] C. van den Doel and J. Smit, *Nucl. Phys.* **B228**, 122 (1983).
- [33] M. F. Golterman and J. Smit, *Nucl. Phys.* **B245**, 61 (1984).
- [34] See Supplemental Material <http://link.aps.org/supplemental/10.1103/PhysRevD.93.081701> for further details of the analysis presented.
- [35] S. Hands, A. Kocic, and J. B. Kogut, *Ann. Phys. (N.Y.)* **224**, 29 (1993).
- [36] R. Pordes *et al.*, *J. Phys. Conf. Ser.* **78**, 012057 (2007).
- [37] I. Sfiligoi, D. C. Bradley, B. Holzman, P. Mhashilkar, S. Padhi, and F. Wurthwein, The Pilot Way to Grid Resources Using glideinWMS, in *WRI World Congress on Computer Science and Information Engineering, Los Angeles, CA* (IEEE, New York, 2009), Vol. 2, pp. 428–432.